ACTA METALLURGICA SLOVACA
2023, VOL. 29, NO. 4, 192-199

RESEARCH PAPER

WEAR AND ADHESION PROPERTIES OF MULTILAYER Ti/TiN, (/TiC)/ TiCN/ TaN THIN FILMS DEPOSITED ON Ti13Nb13Zr ALLOY BY CLOSED FIELD UNBALANCED MAGNETRON SPUTTERING

Ali Kemal Aslan[1], Erkan Bahçe[2]

[1] Department of Metal and Machinery Technologies, Tunceli Vocational School, Munzur University, Tunceli, Turkey, ORCID ID: https://orcid.org/ 0000-0001-6390-9009
[2] Department of Mechanical Engineering, Faculty of Engineering, İnönü University, Malatya, Turkey, ORCID ID: https://orcid.org/0000-0001-5389-5571

*Corresponding author: akaslan@munzur.edu.tr, tel.: +90 428 213 1794, Tunceli Vocational School / Munzur University, 62000, Tunceli, Turkey

Received: 03.10.2023
Accepted: 14.11.2023

ABSTRACT

Ti13Nb13Zr alloy stands out as an alternative to Ti6Al4V alloy for orthopaedic joint implant applications due to its low modulus of elasticity, high mechanical properties, high corrosion resistance, high biocompatibility and low modulus of elasticity, as well as containing no cytotoxic elements. In this study, Ti13Nb13Zr alloy was coated with TiN/TiC/TiCN/TaN multilayer thin films by pulsed-dc CFBUMS method to increase wear resistance and improve surface properties. Characterization of the deposited films were conducted by XRD, SEM, AFM, pin-on-disk, progressive scratch experiments. As a result, it is observed that all the coatings enhanced the tribological properties of the Ti13Nb13Zr alloy surface. The 20-layer TiN/TiC/TiCN/TaN multilayer coatings gave the best results for wear resistance and adhesion properties. Enhancing the interlayer number resulted in increased wear and adhesion resistance. In addition, it was determined that using TiC instead of TiN in the interlayers gave higher results regarding adhesion, wear, and mechanical properties.

Keywords: Biomaterial, Ti13Nb13Zr, Multilayer Coating, Wear, Adhesion.

INTRODUCTION

Titanium alloys are preferred in biomedical applications due to their features as high corrosion resistance, osteointegration, and low density [1]. Ti6Al4V alloy is the most widely used alloy in this field, but the results obtained from clinical studies have shown that the V and Al elements contained in the alloy have cytotoxic effects [2-4]. It has been determined that the ions of these elements released from the alloy into the body fluid accumulate in the tissues and their surroundings and cause various tissue inflammation and osteomalacia [5-6]. While Ti13Nb13Zr alloy has mechanical properties close to Ti6Al4V alloy, it does not contain cytotoxic components [7]. In addition, due to its lower elastic modulus compared to other biometals, orthopaedic joint implants are prone to reduce the strain shield effect in load-bearing applications [8]. However, the use of the alloy in this area is restricted due to its disadvantageous properties as low wear resistance and fatigue resistance in a frictional environment [9].

Various studies have been carried out to improve the surface properties of the Ti13Nb13Zr alloy. Most of these studies aimed at improving surface properties by oxidizing the alloy surface with methods such as PEO [10-15]. As a result of these studies, coatings with increased osteointegration and corrosion resistance were made by coating TiO_2 layers on the surface. In addition, electrophoretic coating studies with hydroxyapatite (HaP) were also carried out to increase the bioactivity of the alloy [9,16]. Apart from these, there are few studies on improving the surface properties of Ti13Nb13Zr alloy by coating by the PVD method. Li et al coated single-layer TiN and multi-layered Ti/TiN coatings on the Ti13Nb13Zr alloy surface by filtered arc deposition method. As a result of their studies, they found that multi-layer Ti/TiN coatings showed much higher resistance to cracking and delamination compared to single-layer TiN coating [17]. Hee et al. coated the surface of the Ti13Nb13Zr alloy with Tantalum using the filtered cathodic arc deposition method to increase the wear and corrosion resistance under load in the biomedical field. Although the corrosion resistance has been significantly increased by coating the surface, the results obtained from the wear test have concluded that the Tantal coating of the alloy caused poor wear resistance [18].

With surface modifications made by depositing multi-layered thin films on various substrate materials, properties such as wear resistance, corrosion resistance, and microhardness can be improved without compromising the properties of the bulk material [19-22]. Thanks to using nitride compounds of transition metals in this area, surfaces with high wear resistance, corrosion resistance, and microhardness could be obtained [23]. Thin films with high adhesion and mechanical stability, with high abrasion and corrosion resistance, could be deposited, via physical vapor deposition (PVD) methods [24]. Coatings produced by this method have been successfully used in the cutting tool industry, microelectronics industry, and recently in the biomedical field [25-31].

Tantalum's excellent biocompatibility, excellent chemical inertness in vivo, and corrosion resistance comparable to noble metals, as well as its suitability for cell adhesion, cell proliferation, and speciation, make its use as a biomaterial very attractive [32-33]. Due to these properties, the use of this metal alone and its

various oxidized, nitride, and carbide components in biomaterials is increasing [34]. TaN ceramic has been researched for biomedical applications due to its high wear resistance, hardness, and more, high corrosion resistance, and very successful results have been obtained [35-38]. TiN ceramic thin films have been used as wear-protective coatings in tribological applications for many years. TiN thin films, which find application in the cutting tool industry, are also used to improve the properties of biomaterials. TiN thin film coatings with thicknesses ranging from 5-60 μm have been applied in orthopaedic joint implants since 1980 [25,39]. As a result of some previous studies, increased microhardness, wear, and corrosion resistance values were obtained in studies where TiC and TiCN thin films were used as interlayers [22,40,41].

In this study, Ti13Nb13Zr alloy was coated with TiN/TiC/TiCN/TaN multilayer thin films by pulsed-dc CFBUMS method to increase wear resistance and improve surface properties. The wear and adhesion properties of deposited thin films in six different coating architectures were investigated.

MATERIAL AND METHODS

Ti13Nb13Zr alloy used as substrate material was purchased as a 20 mm diameter and 1 m long bar (Baoji Future Titanium Company). The chemical composition ratios by weight specified in the ASTM F-1713 standard and the chemical composition ratios by weight of the alloy used in the study are given in **Table 1**.

Ti13Nb13Zr alloy was cut in the form of discs with the laser cutting method with the dimensions of 2.5 mm x 20 mm by laser cutting method. Then, rough surface grinding was applied to the regions which contacted with laser ion beam to eliminate the possible heat treatment effect. Before the deposition process, all the sample surfaces were grinded with respectively 120, 600, mesh SiC emery paper and were polished 1000, 2000 and 2500 mesh SiC emery paper, and then ultrasonically cleaned in ultrapure water for 15 minutes.

Table 1 Chemical composition of the used alloy and ASTM standard

	Ni	C	H	Fe	O	Nb	Zr	Ti
ASTM	0.05	0.08	≤ 0.012	≤ 0.25	≤ 0.15	≤ 12.5-14	≤ 12.5-14	Balance
Used Alloy	0.02	0.03	0.002	0.10	0.08	13.2	13	Balance

The multilayer coating process was conducted using a pulsed-dc closed-field unbalanced magnetron sputtering system which has four targets (Teer Coatings Ltd.). To examine the tribological and adhesion properties of using different interlayers and the period of interlayers, multilayer thin films were deposited in 6 different coating architectures. Uncoated sample was coded as C0, the architectures and coding of the coatings are given in **Fig. 1**.

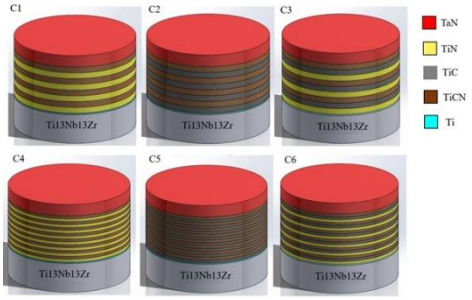

Fig. 1 Schematic presentation of the coating architectures

A thin titanium adhesion layer was first deposited to ensure adhesion to the substrate surface. The TaN layer was deposited as the top layer in all coatings. Tantalum was chosen as the top layer component due to its excellent biocompatibility, the fact that it does not cause any toxic effects when released into the body fluid, and the high wear and corrosion resistance of TaN ceramics [35-38]. Previous studies have been reported TiN and TiC mono or multilayer coatings showed good results in terms of wear and corrosion resistance [25,39]. Moreover, similar results were obtained in previous studies using TiN/TiCN and TiC/TiCN as intermediate layers [22,40]. Therefore, in this study, TiN, TiC, and TiCN components were selected in repeating intermediate layers in different combinations. In the interlayers, three different coating architectures were formed by depositing (TiN/TiCN) x4, (TiC/TiCN) x4, and (TiN/TiC/TiCN) x4 components. To examine the effects of the period of interlayers on the tribological and adhesion properties, the depositing time was halved same time the interlayer period was doubled, and three different coatings were made. The number of intermediate layers was determined so that the total coating thickness could be approximately 2.5-3 πm. To make thickness analyses and morphological examinations of the coatings, coatings were deposited on glass substrates too in all coating processes. The coating parameters are given in **Table 2**.

The phase analysis of the deposited thin films was determined by X-ray diffraction experiments at a scanning speed of 2.0º min^{-1} degree at a wavelength of λ = 0.132 Å and a rotation angle range of 2θ = 3-80° by XRD (Rigaku, USA). Microhardness tests were carried out on a Mitutoyo HM brand microhardness measuring device (Japan) under 125 gf load for 15 seconds, using a diamond pyramid tip with a 136° apex angle, applying a static load. An atomic force microscope (PARK XE, Korean) was used to determine the surface roughness of the samples. The tribological properties of the coatings were determined using a 6.25 mm diameter alumina sphere as the counter material in a pin-on-disc device (Teer Pod, UK) at 25 °C and 45% humidity. Progressive scratch tests were examined to determine the adhesion of the multilayer coatings to the substrate. Experiments were conducted using a Revetester CSM Instruments scratch tester with 10 mm/min feed at 10 N/s load increase rate at 0.2N initial load. SEM investigations were performed to investigate the microstructure and the morphology of the deposited multilayer thin films (Zeiss Evo Ls 10).

Table 2 Coating Parameters

	Layer					
Parameter	**İon Cleaning**	**Ti**	**TiN**	**TiC**	**TiCN**	**TaN**
Work Pressure (Pa)	2.66	3.34	3.34	3,34	3.34	3.34
Ti Target Current (A)	-	4.5	4.5	4.5	4.5	4.5
C Target Current (A)	-	-	-	2	2	-
Ta Target Current (A)	-	-	-	-	-	4
Flow rate of N_2 (sccm)	-	-	7	-	7	14
Flow rate of Ar (sccm)	14	7	7	7	7	7
Bias Voltage (V)	-800	-70	-70	-70	-70	-70
Deposition Time (min)	30	10	8	8	8	70

RESULTS AND DISCUSSION

Microstructure of the coatings

The thicknesses of the thin films deposited on the Ti13Nb13Zr alloy substrate were calculated on the section view of the films deposited on the glass substrate by using SEM (**Table 3**).

Table 3 Thicknesses of the coatings

Coating	**C1**	**C2**	**C3**	**C4**	**C5**	**C6**
Thickness (µm)	2.36	2.41	2.54	2.45	2.52	2.72

In **Fig. 2**, the SEM image taken from the cross-section of the C6 coating deposited on the glass substrate is given, and the coating layers can be seen clearly. It is seen that the TiN/TiC/TiCN/TaN thin films deposited on the Ti13Nb13Zr alloy substrate grow in a dense and crystalline structure.

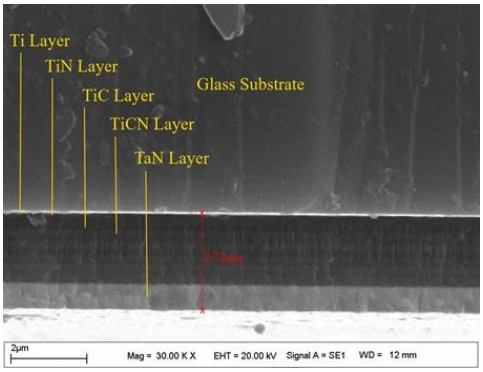

Fig. 2 Cross-sectional SEM image of C6 coating deposited on glass substrate

XRD patterns of the bare Ti13Nb13Zr alloy and coated samples are shown respectively in **Fig. 3** and **Fig. 4**. As a result of XRD analysis, the presence of α' and β titanium phases was determined in Ti13Nb13Zr alloy, a beta titanium alloy. It is usual for the Ti13Nb13Zr alloy to contain α' phases because the β phase is proportionally more in its structure [42-44].
XRD results of the all multilayer coatings showed crystalline structure. Since the thickness of the all thin films deposited on the Ti13Nb13Zr alloy is less than 5 µm, the existence of α' and β titanium phases were detected in all the coatings. A sharp peak of α-TaN (110) bcc phase was observed at 38.4° degrees for all coatings. Besides, orthorhombic base centred Ta_4N (110) phase, face centred cubic TaN (111), and $TaN_{1.13}$ (220) phases were detected at approximately the same intensities in all coatings [42,43,45,46]. XRD patterns of the coatings showed stable crystallinity of TaN phases. This result can be interpreted as the Ta conversion temperature, which is 300 °C, is not exceeded during the coating process [43,45]. It was understood that all the coatings have the same phases due to all the TaN layer's coating parameters being the same. This result indicates that the plasma formed in the coating process was in a homogeneous structure and maintains its homogeneous structure during its deposition on the substrate.

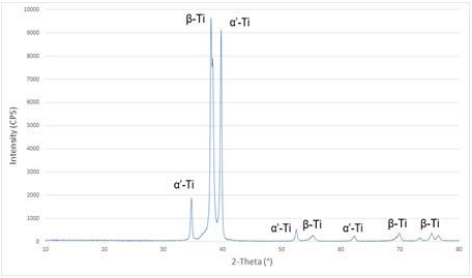

Fig. 3 XRD pattern of Ti13Nb13Zr alloy

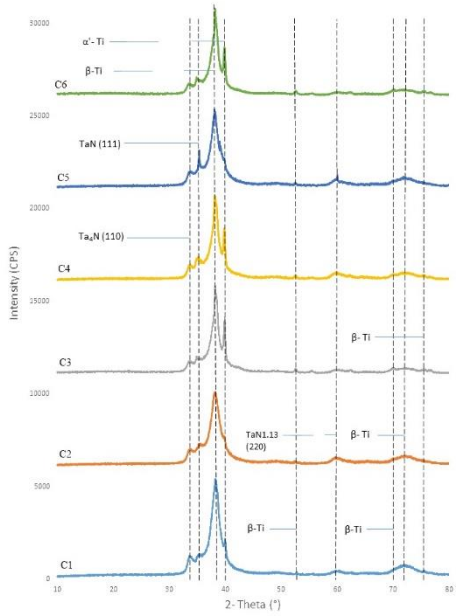

Fig. 4 XRD patterns of the coatings

Hardness and surface roughness of the coatings

Microhardness and surface roughness of the uncoated Ti13Nb13Zr alloy and coated samples were given in Table 4. Although the top layer was TaN deposited with the same coating parameters in all coating architectures, it was understood that the thin films deposited TiN/TiC/TiCN in the interlayers gave higher hardness values. Besides, it is observed that TiC/TiCN interlayer provided higher microhardness compared to the TiN/TiCN interlayer. In multilayer thin film coatings, the microhardness value is affected by the hardness and elastic modulus of the substrate material, as well as by the stiffness and modulus of elasticity of the thin films deposited in the interlayers [47]. Since the C atom causes more distortion in the titanium lattice structure compared to the N atom, the microhardness of the TiC film is higher than that of TiN [23,25]. Accordingly, a higher microhardness value was obtained for C2 coating than for C1 coating. Similarly C5 coating showed higher microhardness compared to C4 coating too. Another finding is that increasing the period of the interlayers had increased the microhardness of all coating architectures. Surface roughness analysis showed similar results to hardness results. The lowest surface roughness value was obtained for the C6 coating. And similarly to hardness results, surface roughness values of the coatings decreased by increasing the period [48].

Table 4 Microhardness and surface roughness of the coatings

Sample	C0	C1	C2	C3	C4	C5	C6
Microhardness (Vickers)	444.60	880.94	989.50	1212.90	1108.03	1212.5	1394.5
Ra (nm)	55.862	25.219	23.458	24.250	20.862	19.208	18.170

As a result of the microhardness experiments, it was observed that although the coating thicknesses of the deposited thin films were close to each other, the microhardness values increased with the increasing period of interlayers in coatings with the same coating architectures. Previous studies have reported that multilayer coatings provide better mechanical properties than that single-layer coatings [48,49]. Also, some studies reported that increasing the layer number increased the hardness [20,21]. It is thought that increasing the layer number was made the dislocation motion more difficult. In addition, when the microhardness results are considered together with the surface roughness results, it is seen that the surface roughness decreases with the increasing number of layers. It is thought that this situation is related to the fact that the nano-sized voids on the coating surface are more filled with the increasing number of layers.

Tribological Behaviour

Tribological properties of the multilayer coatings deposited on the Ti13Nb13Zr alloy was evaluated by pin-on-disk experiments. The wear rate of the uncoated Ti13Nb13Zr alloy and coated samples were calculated according to the equation given below [50]:

$$W_r = \frac{V}{F_n \cdot S} \quad (1.)$$

Where the Wr is the calculated wear rate (mm^3. $N^{-1}.m^{-1}$), V is the wear volume (mm^3), F is the normal load (N) and the S is the sliding distance (m). Coefficients of the friction (COF) and the wear rates of the samples are given in **Table 5**.

Table 5 COF and wear rates of the coatings

Sample	C0	C1	C2	C3	C4	C5	C6
COF	0.508	0.199	0.152	0.163	0.146	0.166	0.128
Wear Rate ($x10^{-7}$) [mm^3/N.m]	571	13.04	7.15	6.86	5.18	4.26	2.29

As a result of pin-on-disk experiments, all the coatings showed a significantly decreased wear rate compared to bare Ti13Nb13Zr alloy. Thanks to the multi-layer coating with ceramic components, the alloy surface has increased microhardness and reduced surface roughness values, thus increasing the wear resistance to a very high value without compromising the mass properties of the alloy [51]. When the wear rates of C1 and C2 coatings, which have the same number of coating layers but different interlayers, are compared to each other, it has been determined that the C2 coating with the TiC/TiCN interlayer gives a lower wear rate than the C1 coating with the TiN/TiCN interlayer. As a result of the wear test carried out under the same conditions, it is expected that the wear resistance of the material with high hardness and low surface roughness will be high compared to the other material [52]. From this point of view, it is understood that the results are in agreement with the microhardness and surface roughness results of the coatings. It has been reported in previous studies that the microhardness and wear resistance values of TiC thin films are higher than TiN thin films, and this is due to the fact that the carbon atom causes more distortion in the titanium lattice compared to nitrogen [23,48]. The wear rate of the C3 coating, which has TiN/TiC/TiCN interlayers, was found as lower than C1 and C2 coatings. It was found that using the TiN/TiC/TiCN interlayers increased the wear resistance approximately twofold compared to using TiN/TiCN interlayers. On the other hand, when TiN/TiC/TiCN interlayer is used alternative to TiC/TiCN interlayer, it is seen that there is not such a broad increase in terms of wear resistance. From this point of view, it has been concluded that the difference between the wear resistance of C1 and C3 coatings is due to the presence of TiC in the interlayers, rather than the use of TiN/TiC/TiCN interlayers.

As a result of the wear test of the C4 coating, which has the same interlayer composition as the C1 coating, a wear rate of 5.18 x 10^{-7} $mm^3.N^{-1}.m^{-1}$ was obtained. Considering that the thicknesses of both coatings are very close to each other, and the interlayer period of the C4 coating is 2 times that of the C1 coating it is understood that the wear resistance increases approximately 2.5 times by doubling the period of interlayers. Similar results were obtained for C5 and C6 coatings compared to C2 and C3. It is thought that by increasing the period of interlayers, the surface roughness and residual stresses decrease, and as a result, the wear resistance increases. The surface roughness results of the coatings support the wear test results in this respect. It has been reported in previous studies that increasing the period of layers in multilayer thin film coatings increases the mechanical properties such as hardness, corrosion resistance, fatigue resistance

as well as wear resistance [24,53]. From this point of view, it is understood that the results obtained in this study are compatible with the literature data. There have been some studies investigating the wear resistance of TaN thin films [20, 21, 47, 52, 54-58]. Westergard et al. reported 14-62 $\mu m^3.N^{-1}.m^{-1}$ wear resistance as a result of the abrasion test of Ta/TaN thin films deposited by the DC magnetron sputtering method with different magnetron power and nitrogen flow rates [54]. Nordin et al. reported a wear rate of 50.10^{-19} $mm^3.N^{-1}.m^{-1}$ for TiN/TaN thin films deposited on Cemented carbide substrate [55]. Chen et al. obtained 0.2 10^{-14} $\mu m^3.N^{-1}.m^{-1}$ wear rate for TaN thin films deposited on Ti6Al4V substrate by DC magnetron sputtering method [57]. Ma et al., on the other hand, found that 19.4 mm^3 wear amount for multilayer Ta/TaN coatings deposited on Co12MoV substrates, stating that multilayer coatings gave the best results in terms of wear and corrosion resistance [21]. When the wear rate obtained in this study is compared with those in the literature data, it is understood that some of them have high and some low wear resistance. Since the mechanical and tribological properties of thin film coatings are affected by many factors coating method, coating parameters, substrate material, coating thickness, and morphology, it is usual for the results to be different [48].

Adhesion properties of the coatings

The progressive load scratch experiments were performed to determine the adhesion properties of the coatings. As a result of the experiments, critical load (Lc) values that depict where the coating is fully deformed were determined, and normal load/friction force graphs were given together with the optical micrographs captured during scratch experiments. **Fig. 5** presents the scratch results of the C1 coating. In the figure, the red curve presents the friction coefficient, and the purple curve the friction force. The critical load of the C1 coating was determined at 13.42 N. It can be seen that at a load of approximately 2 N an adhesive failure occurred in a part of the top layer of the coating, and the fluctuation of the friction coefficient curve at this load confirms this. The fact that the color of the region where the adhesive failure occurred is brown, which is the colour of the TiCN layer, indicates that the fracture occurred on the TaN layer. Also, there is a spallation failure of the TaN layer in the scratch band above the adhesive failure region, but this spallation hasn't continued. When the optical images are examined, it is understood that little capillary cohesive failures occurred on the upper edge, and adhesive failures occurred on the lower edge of the scratch band. It is thought that the occurrence of different damage mechanisms on the edges in this way is due to the slope on the surface. It can be seen that abrasive wear scratches and grooves are formed in the inner part of the scratch band parallel to the scratch direction, and there are little abrasive wear particles in these grooves. With the increasing load and progress, it was understood that the top layer started to break down at approximately 10 N loading in the scratch band, the coating was fully removed at a load of 13.42 N, and the pin reached the substrate material. At the beginning of the scratch test of the C2 coating, it is observed that the TaN layer is separated at about 3N loading, but this separation remains localized (**Fig. 6**). In the image taken under a 10 N load, it can be seen that there are little capillary cohesive scratches and a small amount of adhesive separation at the edges of the scratch band, abrasive wear particles inside the scratch band, and partial capillary cracks on the layer. It is understood that with increasing the load, the number of capillary cracks in the scratch tape and the cohesive scratches on the tape edge increase, and the width of the abrasive wear grooves along the lower edge of the scratch tape relative to the page. It is concluded that the dominant damage mechanism in this coating layer is cohesion cracks, and the coating maintains its integrity up to the critical load value.

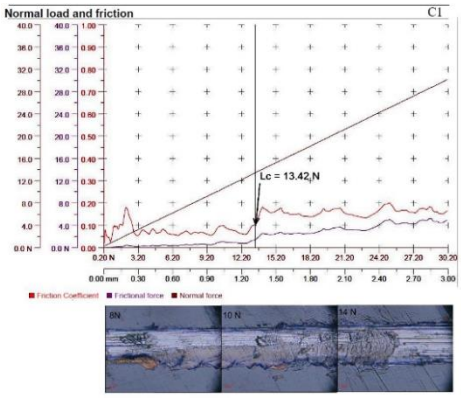

Fig. 5 Scratch behaviour of C1 coating

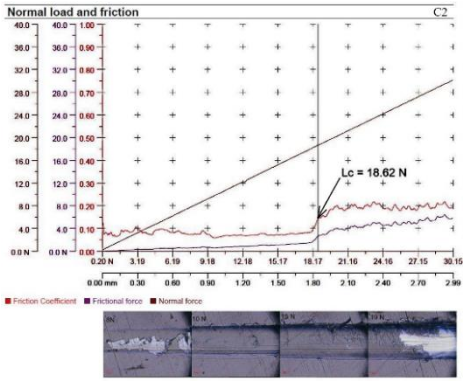

Fig. 6 Scratch behavior of C2 coating

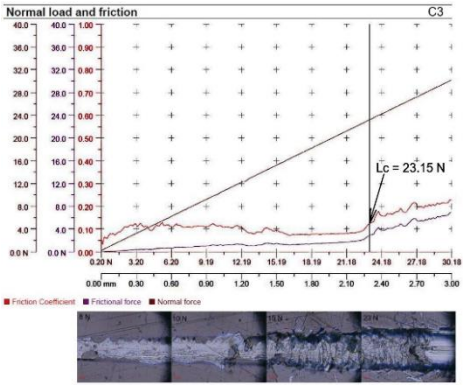

Fig. 7 Scratch behavior of C3 coating

Fig. 7 represents the scratch results of the C3 coating. When the figure is studied, it is understood that the scratch trace continues as abrasive failure inside the scratch band, except for the cohesive failures that occurred around the scratch band from the adhesive failure zone at 8 N loading to the adhesive failure zone at 10 N loading. With the increase of the applied load, it was observed that the coating layer started to crack by forming deep cohesive scratches from the periphery of the scratch band to the inside. As a result of increasing the applied load, the coating was fully deformed, and the tip reached the substrate material at 23.15 N loading. It can be concluded that from the 15 N load till the critical load, the coating has spallation cracks.

The scratch test results of the C4 coating, which has the same coating architecture as the C1 coating but twice the number of interlayers, are given in **Fig. 8**. When the optical micrographs are investigated, it can be seen that both 8 N and 10 N load, brown colored abrasive wear grooves were seen in the scratch band. In these regions, it is understood that the TaN layer, has detached, and the TiCN layer is present. The dark black region in the image taken at 10 N loading belongs to the TiC layer under the TiCN layer, and it has been determined that the TiCN layer has undergone adhesive failure in this region. As a result of the increase of the load, it can be seen that the adhesive wears occurring around the scratch band deepen and reach the TiC layer, while the cohesive scratches and abrasive wear products increase inside the scratch band. The critical load value for this coating was found to be 23.1 N, and spallation cracks were observed just before reaching this value.

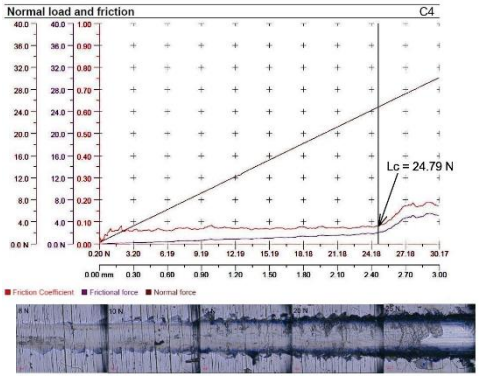

Fig. 8 Scratch behavior of C4 coating

When the scratch results of the C5 coating were studied (**Fig. 9**), it can be seen that, unlike the other coatings, no delamination damage was observed around the scratch band, except for capillary scratches, up to 10 N loading. It is seen that the TaN layer undergoes adhesive failure at approximately 12 N loading, confirming this by the fluctuation in the normal load curve. After that, it is seen that while the capillary scratches around the scratch band caused damage to the coating by the chipping mechanism, spallation cracks began within the scratch band. The critical load value at which this coating layer removed completely has been determined as 26.64 N, and it is seen that small spallation on the surface have preserved their form before reaching the substrate material, and they have suddenly ruptured at the critical load value. When the friction coefficient curve is examined, it is seen that it is in a stable structure up to 20 N loading, except for approximately 12 N loading. This result can be interpreted as the homogeneity and stability of the coating is higher than the previous coatings.

As a result of the scratch test of the C6 coating, which has the highest number of interlayers, it is seen that there is an adhesion break at a load value of approximately 8 N on the coating surface (**Fig. 10**). Besides, adhesive detachments along the scratch band, cohesive scratch damages, and abrasive wear scratches were observed inside the tape. Except for an adhesive failure formed at approximately 24 N; from 15 N to 30.03 N loading, it can be seen that the coating failure mechanism is chipping at the edges of the scratch tape and spallation cracks in the scratch tape. When the optical images and the friction coefficient curve data are considered together, it is seen that this coating has a homogeneous and stable structure.

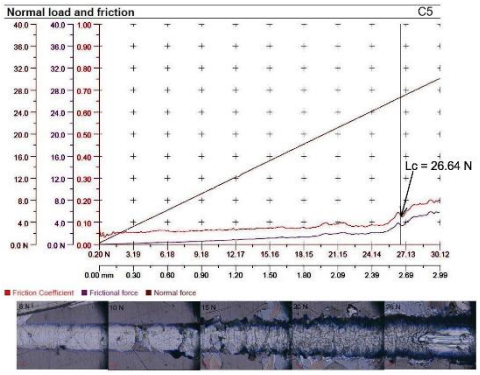

Fig. 9 Scratch behavior of C5 coating

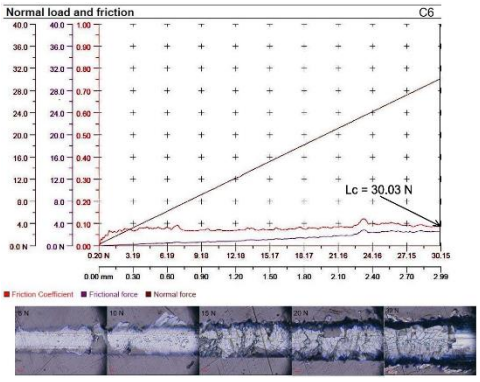

Fig. 10 Scratch behavior of C6 coating

According to the critical load values (Table 6.), the C6 coating showed the best adhesion to the Ti13Nb13Zr substrate. When the adhesion strength of the C3 coating, which has the same interlayer structure as the C6 coating, is compared, it has been determined that doubling the period of interlayers significantly increases the adhesion strength. From this point of view, when the C1-C4 coatings and C2-C5 are compared among themselves, it has been determined that halving the deposition time of each intermediate layer, and doubling the period of intermediate layers, resulted in increasing the adhesion strength. Residual stresses occur in multilayer thin film coatings due to the mismatch of the lattice parameters and modulus of elasticity of the substrate material and the thin films deposited on it [59]. Besides, the different thermal expansion coefficients between the substrate and thin films also cause residual stresses. Thanks to the different modulus of elasticity of TiN/TiC and TiCN used as interlayers

in this study, it is thought that residual stresses are reduced by providing a gradual transition from the substrate material to the TaN coating layer. By increasing the number of interlayers, both the tensile stresses between the substrate and the coating were reduced, and the contact surface of the applied force in the scratch test was increased, thus increasing the scratch resistance of the coating [60]. Another finding obtained from scratch experiments is that TiC deposition with TiCN in the interlayers provides higher adhesion than TiN deposition. This can be explained by TiCN making more coherent bonding on TiC than TiN. On the other hand, depositing the triple TiN/TiC/TiCN interlayer showed more adhesion resistance than the other two coatings. From this, it can be concluded that when the TiC/TiCN layer is deposited on the TiN layer, a coherent interface is formed between TiN and TiC, which have a similar lattice structure, thus increasing the adhesion of the coating to the substrate [61,62].

Table 6 Critical load values of the coatings

Coating	C1	C2	C3	C4	C5	C6
Critical Load (Lc) [N]	13.42	18.62	23.15	24.79	26.64	30.03

CONCLUSIONS

Six different multilayer TiN/TiCN/TaN coatings deposited on biomedical Ti13Nb13Zr alloy by CFUBMS system. As a result of the characterization experiments following conclusions were determined:

- The 20-layer TiN/TiC/TiCN/TaN multilayer coatings gave the best results for wear resistance and adhesion properties.
- It was found that the deposition of TiC/TiCN in interlayers provides higher wear resistance and adhesion properties than TiN/TiCN.
- Doubling the period of interlayers without changing the coating thicknesses significantly improves the surface properties of the coatings.
- It has been determined that the mechanical properties of the alloy surface is considerably increased thanks to the multilayered TiN/TiC/TiCN/TaN coatings deposited on the Ti13Nb13Zr alloy.
- As a result of further experimental studies, since the 20-layer TiN/TiCN coating on the Ti13Nb13Zr alloy surface increases the wear resistance and fatigue strength, it is thought that this alloy will pave the way for its use as a load bearing element in biomedical applications.

Acknowledgments: This scientific research has financially supported from Scientific Research Project Committee of İnonu University (No: FKP 2020-2092) and Ottoman Group Implant CO. The authors are gratefully for these supports.

REFERENCES

1. L.C. Zhang, L.Y.Chen: Advanced Engineering Materials, 21(4), 2019, 1801215. https://doi.org/101002/adem.201801215.
2. D. Cadosch, E. Chan, O.P. Gautschi, L. Filgueira: Journal of Biomedical Materials Research Part A , 91A(4), 2009, 1252-1262. https://doi.org/10.1002/jbm.a.32625.
3. C.C. Gomes et al.: Genetics and Molecular Biology, 34(1), 2011, 116-121. https://doi.org/10.1590/S1415-47572010005000118.
4. Y. Zhang et al.: Colloids and Surfaces B: Bipinterfaces, 169, 2018, 366-374. https://doi.org/10.1016/j.colsurfb.2018.05.044.
5. Y. Okazaki, E. Gotoh. Biomaterials. 26, 2005, 11-21. https://doi.org/10.1016/j.biomaterials.2004.02.005.
6. J.J. Jacobs et al.: The Journal of Bone and Joint Surgery, 80(A), 1998, 1447-1458. https://doi.org/ 10.2106/00004623-199810000-00006.
7. K. Wang: Materials Science and Engineering A. 213, 1996, 134-137. https://doi.org/10.1016/0921-5093(96)10243-4.
8. Y. Li, C. Yang, H. Zhao, S. Qu, X. Li, Y. Li: Materials. 7, 2014, 1709-1800. https://doi.org/10.3390/ma7031709.
9. M. Bartmanski et al.: Ceramics International, 43, 2017, 1820-1829. https://doi.org/10.1016/j.ceramint.2017.06.026.
10. A. Kazek-Kesik, G. Dercz, K. Suchanek, I. Kalemba-Rec, J. Piotrowski, W. Simka: Surface & Coatings Technology, 276, 2015, 59-69. https://doi.org/10.1016/j.surfcoat.2015.06.034.
11. A. Kazek-Kesik, M. Krok-Borkowicz, G. Dercz, A. Donesz-Sikorska, E. Pamula, W. Simka: Electrochimica Acta, 204, 2016, 294-306. https://doi.org/10.1016/j.electacta.2016.02.193.
12. S. Lederer, P. Lutz, W. Fürbeth: Surface & Coatings Technology, 335, 2018, 62-71. https://doi.org/10.1016/j.surfcoat.2017.12.022.
13. D.A.G. Perez et al.: Journal of Alloys and Compounds,. 812, 2020, 152116. https://doi.org/10.1016/j.jallcom.2019.152116.
14. M. Sowa et al.: Materials Science and Engineering C , 49, 2015,159-173. https://doi.org/10.1016/j.msec.2014.12.073.
15. E. Urbanczyk, A. Krzakala, A. Kazek-Kesik, J. Michalska, A. Stolarczyk, G. Dercz, W. Simka: Surface & Coatings Technology, 291, 2016, 79-88. https://doi.org/10.1016/j.surfcoat.2016.02.025.
16. M. Jażdżewska, B. Majkowska – Marzec: Advances in Materials Science, 4 (54), 2017, 5-13. https://doi.org/10.1515/adms-2017-0017.
17. J. Li, H. Zheng, T. Sinkovits, A.C. Hee, Y. Zhao: Applied Surface Science, 355, 2015, 502-508. https://doi.org/10.1016/j.apsusc.2015.07.126.
18. A.C. Hee, P.J. Martin, A. Bendavid, S.S. Jamali, Y. Zhao: Wear, 400-401, 2018, 31-42. https://doi.org/10.1016/j.wear.2017.12.017.
19. X. Guan, Y. Wang, G. Zhang, X. Jiang, L. Wang, Q. Xue: Tribology International, 106, 2017, 78-87. https://doi.org/10.1016/j.triboint.2016.10.036.
20. E. Bahçe, N. Çakır: Reviews on Advanced Materials Science 58, 2019, 271-279. https://doi.org/10.1515/rams-2019-0036.
21. G. Ma, G. Lin, S. Gong, X. Liu, G. Sun, H. Wu: Vacuum. 89, 2013, 244-248. https://doi.org/10.1016/j.vacuum.2012.05.024.
22. J. Zheng, J. Hao, X. Liu, Q. Gong, W. Liu: Surface & Coatings Technology, 209, 2012, 110-116. https://doi.org/10.1016/j.surfcoat.2012.08.045.
23. H.O. Pierson: *Handbook Of Refractory Carbides and Nitrides*, 1st. ed. New Jersey: Noyes Publications, 1996.
24. T. Vieira, J. Castanho, C. Louro: Hard Coatings Based on Metal Nitrides, Metal Carbides and Nanocomposite Materials: PVD Process and Properties, In: *Materials Surface Processing By Directed Energy Techniques*, Pauleau Y. eds., United Kingdom, Elsevier, 2006, 537-572.
25. T. Schmitz: [Dissertation]. Würzburg: Bayerischen Julius-Maximilians-Universität; 2016. urn:nbn:de:bvb:20-opus-144825 (2016).
26. G. Skordaris et al.: Surface & Coatings Technology, 307, 2016, 452-460. https://doi.org/10.1016/j.surfcoat.2016.09.026.
27. D.M.D. Reis, S. Rzepka, K. Hiller: Microelectronics Reliability, 88-90, 2018, 835-839. https://doi.org/10.1109/TRANSDUCERS.2019.8808421.
28. Ł. Łapaj, J. Wendland, J. Markuszewski, A. Mroz, T. Wisniewski: Journal of The Mechanical Behaviour of Biomedical Materials, 55, 2015, 127-139. https://doi.org/10.1016/j.jmbbm.2015.10.012.
29. M. Geetha, A.K. Singh, R. Asokamani, A.K. Gogia: Progress in Materials Science. 54, 2009, 397-425. https://doi.org/10.1016/j.pmatsci.2008.06.004.
30. C. Thorwarth et al.: Acta Biomaterialia, 6, 2010, 2335-2341. https://doi.org/10.1016/j.actbio.2009.12.019.
31. A. Nouri, C. Wen: Introduction to surface coating and modification for metallic biomaterials, In: *Surface Coating and Modification of Metallic Biomaterials*, Wen C. eds., UK: Woodhead Publishing, 2015, 3-60.
32. V.K. Balla, S. Bose, N.M. Davies, A. Bandyopadhyay: Biological and Biomedical Materials, 62(7), 2010, 61-64. https://doi.org/10.1007/s11837-010-0110-y.
33. Y.X. Leng, J.Y. Chen, P. Yang, H. Sun, J. Wang, N. Huang: Nuclear Instruments and Methods in Physics Research B, 242, 2006, 30-32. https://doi.org/10.1016/j.nimb.2005.08.002.
34. C. Balagna, M.G. Faga, S. Spriano: Materials Science and Engineering C, 32, 2012, 887-895. https://doi.org/10.1016/j.msec.2012.02.007.
35. S.K. Kim, B.C. Cha: Thin Solid Films, 475, 2005, 202- 207. https://doi.org/10.1016/j.tsf.2004.08.059.
36. T. Schmitz, C. Hertl, E. Werner, U. Gbureck, J. Groll, C. Moseke: Surface & Coatings Technology, 216, 2013, 46-51. https://doi.org/10.1016/j.surfcoat.2012.11.021.
37. A. Jara, B. Fraisse, V. Flaud, N. Frety, G. Gonzalez: Surface & Coatings Technology, 309, 2017, 887-896. https://doi.org/10.1016/j.surfcoat.2016.10.067.
38. Ö. Baran, E. E. Sükürоğlu, İ. Efeoğlu, Y. Totik Journal of Adhesion Science and Technology, 30 (20), 2016, 2188-2200.

https://doi.org/10.1080/01694243.2016.1176662.
39. I. Gotman, E.Y. Gutmanas, G. Hunter: Wear-Resistant Ceramic Films and Coatings, In: Ducheyne P. eds. *Comprehensive Biomaterals*, United Kingdom: Elsevier, 2011, 127-155.
40. Y. Yang, W. Yao, H. Zhang: Surface & Coatings Technology, 205, 2010, 620-624. https://doi.org/10.1016/j.surfcoat.2010.07.058.
41. P.V. Badiger, V. Desai, M.R. Ramesh: Transactions- Indian Institute of Metals, 70(9), 2017, 2459-2464.
https://doi.org/10.1007/s12666-017-1107-9.
42. D. Li et al.: Royal Society of Chemistry Advances, 4, 2014, 10133.
https://doi.org/10.1039/c3ra46734a.
43.A. Zaman: [Dissertation]. Arlington: University of Texas;https://ui.adsabs.harvard.edu/abs/2014PhDT.49Z, 2014.
44. K. Valetti, A. Subrahmanyam, S.V. Joshi, A.R. Phani, M. Passacantando, S. Santucci Journal Of Physics D: Applied Physics, 41, 2008, 045409. https://doi.org/10.1088/0022-3727/41/4/045409.
45. X. Liu, G.J. Ma, G. Sun, Y.P. Duan, S.H. Liu: Applied Surface Science, 258, 2011, 1033-1037. https://doi.org/10.1016/j.apsusc.2011.08.116.
46. J. Corona-Gomez, T.A. Jack, R. Feng, Q. Yang: Materials Characterization, 182, 2011, 111516. https://doi.org/10.1016/j.matchar.2021.111516.
47. D.M. Mattox: *Handbook Of Physical Vapor Deposition (PVD) Processing: Film Formation, Adhesion, Surface Preparation and Contamination Control*, 1st. ed., New Jersey: Noyes Publications, 1998.
48. M.Z. Abdullah, A.N. Abdullah, M.H. Othman, A. Morat, M.A. Ahmad: Advanced Materials Research, 2015, 1133, 99-102.
https://doi.org/10.4028/www.scientific.net/AMR.1133.99.
49. Y.H. Yang, D.J. Chen, F.B. Wu: Surface & Coatings Technology, 303, 2016, 32-40. https://doi.org/10.1016/j.surfcoat.2016.03.034.
50. K. Holmberg, A. Matthews: *Coatings Tribology: Properties, Mechanisms, Techniques and Applications in Surface Engineering*, 2nd. ed., United Kingdom: Elsevier Science & Technology, 2009.
51. B.J. McEntire, B.S. Bal, M.N. Rahaman, J. Chevalier, G. Pezzotti: Journal of the European Ceramic Society, 35, 2015, 4327-4369.
https://doi.org/10.1016/j.jeurceramsoc.2015.07.034.
52. P. Tan et al.: Tribology International, 133, 2019, 126-135.
https://doi.org/10.1016/j.triboint.2019.01.001.
53. R.J.K. Wood, J.A. Wharton: Coatings for tribocorrosion protection. In: *Tribocorrosion of Passive Metals and Coatings*, Landolt D, Mischler S, eds. , United Kingdom: Woodhead Publishing Limited, 2011, 296-333.
54. R. Westergard, M. Bromark, M. Larsson, P. Hedenqvist, S. Hogmark: Surface & Coatings Technology, 97, 1997, 779-784.
https://doi.org/10.1016/S0257-8972(97)00338-1.
55. M. Nordin, M. Larsson, S. Hogmark: Surface & Coatings Technology, 106, 1997, 234-241. https://doi.org/10.1016/S0257-8972(98)00544-1.
56. L. Gladczuk, A. Patel, J.D. Demaree, M. Sosnowski: Thin Solid Films, 476, 2005, 295- 302. https://doi.org/10.1016/j.tsf.2004.10.020.
57. R. Chen, J.P. Tu, D.G. Liu, Y.L. Yu, S.X. Qu, C.D. Gu: Surface & Coatings Technology, 206, 2012, 2242- 2248.
https://doi.org/10.1016/j.surfcoat.2011.09.072.
58. A. Aryasomayajula, K. Valleti, S. Aryasomayajula, D.G. Bhat: Surface & Coatings Technology, 201, 2006, 4401-4405.
https://doi.org/10.1016/j.surfcoat.2006.08.085.
59. L. Kara, T. Küçükömeroğlu, Ö. Baran, İ. Efeoğlu, K. Yamamoto: Metallurgical and Materials Transactions A, 45, 2014, 2123-2131.
https://doi.org/10.1007/s11661-013-2148-2.
60. H.K. Kim, S.M. Kim, S.Y. Lee: Coatings, 12, 2022, 1025.
https://doi.org/10.3390/coatings12071025.
61. K. Yalamanchili et al. : Acta Materialia, 121, 2016, 396–406.
https://doi.org/10.1016/j.actamat.2016.07.006.
62. M. Bielawski, K. Chen: Surface Effects and Contact Mechanics, IX, 2009, 85-94. https://doi.org/10.2495/SECM090081.